



Measuring electrical current during scanning probe oxidation

F. Pérez-Murano, C. Martn, N. Barniol, H. Kuramochi, H. Yokoyama, and J. A. Dagata

Citation: *Applied Physics Letters* **82**, 3086 (2003); doi: 10.1063/1.1572480

View online: <http://dx.doi.org/10.1063/1.1572480>

View Table of Contents: <http://scitation.aip.org/content/aip/journal/apl/82/18?ver=pdfcov>

Published by the [AIP Publishing](#)



Re-register for Table of Content Alerts

Create a profile.



Sign up today!



Measuring electrical current during scanning probe oxidation

F. Pérez-Murano^{a)} and C. Martín

Institut de Microelectrònica de Barcelona (IMB-CNM-CSIC), Campus de la Universitat Autònoma de Barcelona, E-01893 Bellaterra, Spain

N. Barniol

Departament d'Enginyeria Electrònica, Universitat Autònoma de Barcelona, E-08193 Bellaterra, Spain

H. Kuramochi and H. Yokoyama

Nanotechnology Research Institute, AIST, 1-1-1 Umezono, Tsukuba, Ibaraki 395-8568, Japan

J. A. Dagata

National Institute of Standards and Technology, Gaithersburg, Maryland 20899-8214

(Received 3 January 2003; accepted 13 March 2003)

Electrical current is measured during scanning probe oxidation by performing force versus distance curves under the application of a positive sample voltage. It is shown how the time dependence of the current provides information about the kinetics of oxide growth under conditions in which the tip–surface distance is known unequivocally during current acquisition. Current measurements at finite tip–sample distance, in particular, unveil how the geometry of the meniscus influences its electrical conduction properties as well as the role of space charge at very small tip–sample distances. © 2003 American Institute of Physics. [DOI: 10.1063/1.1572480]

Local oxidation using scanning probe microscopy (SPM)¹ is a convenient technique for the fabrication of nanometer-scale structures, with applications in fields such as nanoelectronics,² nano-optics,³ and nanomechanics.⁴ Voltage applied between a conductive SPM tip and the positively biased substrate results in the formation of a highly nonuniform electric field, E . The E field attracts a stable water meniscus to the tip–sample junction, creates oxyanions from water molecules, and transports these oxyanions through the growing oxide film. This leads to oxidation of the substrate on a scale determined by the dimensions of the water meniscus. Despite the inherent simplicity of this scheme, a complete understanding of the kinetics and mechanism of SPM oxidation is still evolving. Specifically, previous work has emphasized aspects of the process either primarily related to the build up of space charge within the oxide film^{5–8} or to control of the meniscus geometry at finite tip–sample distances by dynamic-mode atomic force microscopy (AFM).^{9,10}

Space-charge buildup within the growing oxide film and the meniscus geometry are inherently coupled phenomena since both affect the total current passing through the tip–sample junction at a given stage of the exposure. Thus far, there have been only two cursory measurements of total current during SPM oxidation.^{11,12} Displacement currents at the onset of the voltage pulse, however, obscured the true junction current during the initial fast-growth stage of oxidation. Hence, ionic and electronic components of the total current could not be resolved. Realization of current measurements that yield meaningful data for transient and steady-state SPM oxide growth conditions⁸ requires a very careful procedure. In this letter, we describe an experimental procedure which allows us to avoid displacement current artifacts.

Measurements are performed by acquiring simultaneously the cantilever deflection response along with the current passing through the tip as a function of z -piezo elongation (i.e., a force versus distance curve and a current versus distance curve). The E field at the tip–sample spacing is very high, inducing a large cantilever bending which produces uncertainty in the estimation of the tip–sample separation. In order to avoid excessive bending of the cantilever, stiff cantilevers ($k \approx 40$ N/m) with n -doped silicon tips have been used. We have not used metal-coated tips in order to avoid deposition events (tip and surface are in mechanical contact at least during the repulsive part of the force curve) and to keep a sharp tip radius whenever possible. Each curve is acquired in a different position of the surface in order to avoid extra effects due to change of local surface properties induced by the realization of previous curves. In all the experiments shown here, p -type silicon samples ($0.1 \Omega \text{ cm}$) with native oxide has been used at 60% ambient relative humidity. Current measurements are performed with a transimpedance amplifier connected to the tip with programmable gains of 1 pA/V and 10 pA/V.

Figure 1 illustrates a typical experimental result. Figure 1(a) is a measurement of cantilever deflection versus Z displacement, as the AFM tip first approaches, and then retracts from, the substrate. Z displacement was performed at a speed of 60 nm/s and with a voltage of 9 V maintained during the entire cycle, thereby eliminating displacement current. An oxide dot is created on the surface at the point of contact, as verified by subsequent AFM imaging of the sample surface. The following regimes are labeled in the figure: (i) Initial deflection of the cantilever due to the electrostatic force between tip and sample; (ii) Overshoot as the unsupported, concave down, cantilever jumps into contact with the surface; (iii) Linear deflection of the supported, concave-up cantilever; and, (iv) Separation of tip and sample in the presence of electrostatic and meniscus forces, followed by pull off of

^{a)}Electronic mail: francesc.perez@cnm.es

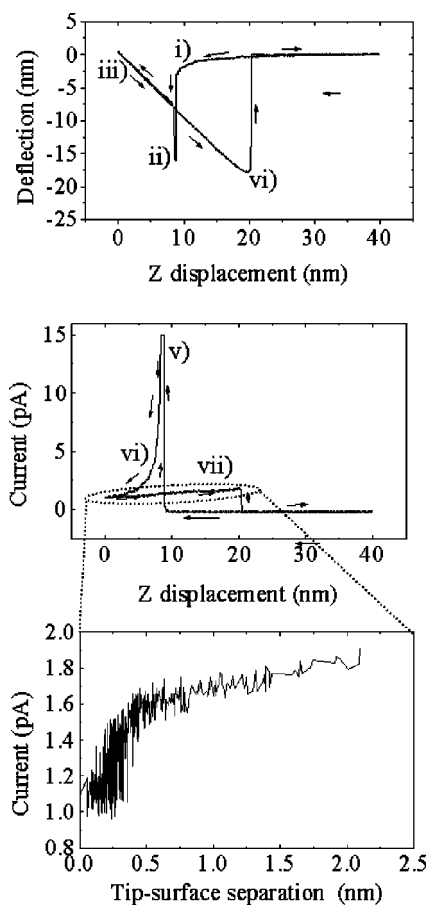


FIG. 1. Simultaneous acquisition of a force-vs- Z displacement curve, (a), and current flowing through the tip-sample junction, (b), under an applied voltage of 9 V (sample positive). The surface is p -type silicon (100) with native oxide and the tip and cantilever is n -doped silicon with force constant of 45.9 N/m. (c) Plot of the current versus tip-sample separation for the retraction part of the curve.

the tip from the sample surface. We have verified that the portion of the approach curve which corresponds to pure electrostatic cantilever bending, regime (i), is well described by $F \approx a \cdot V/Z$ over a wide range of voltage V and Z -displacement range and speed. In fact, the fitting of the data according to V/z and $(V/z)^2$ in this range of V and z , where the surface area of the (planar) cantilever dominates the electrostatic interaction, are very similar. To compare this simple interaction to the more complicated electrostatic + ionic + meniscus force acting to resist tip pull off, regime (iv), we must use the actual tip-sample separation, s . For stiff cantilevers this can be done reliably, since $s = (d - Z)$ which corresponds to the deviation from linearity near pull off (d is the cantilever deflection). The actual measured pull-off force is well described by $F \approx b \cdot V/s$, with $b = 0.3 \cdot a$. Evidently, the presence of a meniscus results in a reduction of the purely electrostatic force experienced by the tip during the approach.

Figure 1(b) presents a simultaneous measurement of the current passing through the tip-sample junction over the Z -displacement cycle. The following regimes are labeled in Fig. 1(b); (v) Initial appearance of the maximum current corresponding to the formation of a water meniscus and the onset of electronic and electrolytic processes; (vi) Time evolution of current when tip and surface are in mechanical con-

tact; and, (vii) Increase of current prior to pull off. Extensive fitting of the experimental current data from 1 to 100 pA for a wide range of voltage indicates that the maximum current through the tip-sample junction, regime (v), can be described by a simple exponential, $I_{\max} \approx \exp(V)$. Additional experiments performed with hydrogen-terminated and native-oxide silicon substrates and with metal-coated AFM tips also confirm that I_{\max} is a junction parameter and does not arise from displacement current.

Figure 1(c) is a graph of current plotted, not as a function of Z displacement as in regime (vii) of Fig. 1(b), but as a function of the actual tip-sample separation, s . Observe that current increases beyond the first 0.5 nm of actual separation. This increase of current during the retraction part of the force versus distance curve can be observed for sufficiently high voltage and Z -displacement speed. Although we can routinely observe a similar qualitative increase in most cases, we find that quantitatively this current increase is a sensitive function of the tip shape and other conditions, such as humidity and surface preparation. Despite this, when the increase of current is observed, it always corresponds to an increase of separation between 0.5 and 2 nm in our experiments. This somewhat unexpected phenomenon must be considered with reference to the reduced interaction force at pull off, $F \approx b \cdot V/s$, discussed herein. A self-consistent explanation for a simultaneous current increase and reduced force within regimes (iv) and (vii) is reorganization of space charge at the tip-substrate junction with increasing separation. The counter charge of the double layer screens the pure electrostatic force, thus reducing the force required to achieve pull-off force once a sufficient restoring force can be built up in the cantilever to begin the separation of the tip and the sample. Once charge separation occurs, ionic current increases because of reduced space charge at the tip-substrate junction.

Since Z displacement is carried out at constant speed, it is straightforward to convert regime (vi) current versus Z -displacement data into current versus time, s , Fig. 2. Analysis of the time evolution of current provides a powerful tool to study oxide-growth kinetics at a series of voltages to within the first few milliseconds of oxidation. The semilog plot, Fig. 2(a), shows that current decay is not an exponential function of time, which indicates that a transient due to displacement current does not dominate the measured current. Moreover, the log-log plot, Fig. 2(b), yields a nonconstant slope. This result, obtained from direct current measurement, is consistent with previous kinetic analysis based on measurement of oxide volume: SPM oxidation does not follow Cabrera-Mott behavior, i.e., self-limiting growth due to oxide thickness, but is, on the other hand, limited by space-charge build up in the oxide film.⁸ Since oxide volume, V_{ox} , is proportional to ionic charge transported across the growing oxide film, the decay parameter extracted from Fig. 2, $I(t) \approx I_{\max} \cdot t^{-\gamma}$, must be related to $V_{\text{ox}} \propto t^{(1-\gamma)}$. Initial analysis of experiments over a wide range of voltage indicates that the proportion of the total current attributable to ionic and electronic components is approximately constant. A detailed treatment of the time evolution of current and its relationship to the volume of the oxide growth will be presented in a future publication.

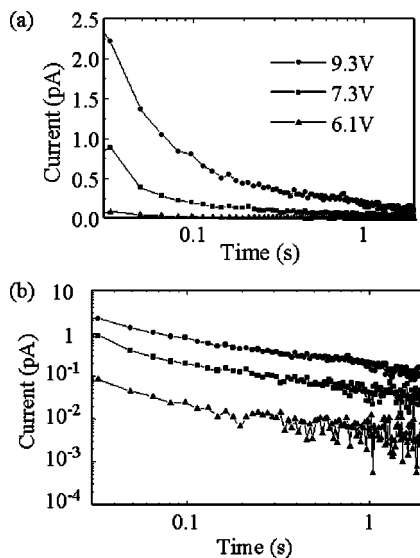


FIG. 2. Current evolution vs time obtained from the repulsive part of the force-vs- Z displacement curves for three different voltages, (a) semi-log and (b) log-log plot. Tip velocity during the approach/retract excursion is 240 nm/s. The surface is p -type silicon (100) with native oxide and the tip and cantilever is n -doped silicon.

Current flow at finite tip-sample separation can be observed on approach curves if the applied voltage is sufficiently large. Previous work using dynamic-mode SPM provided direct evidence for a threshold for voltage-induced meniscus formation, the stability of the meniscus during meniscus elongation, and its effect on oxide growth rate.^{10,13} Figure 3(a) is a series of force versus Z displacement curves obtained at different voltages. The approach was performed in a way that the tip does not make contact with the surface. This prevents the flowing of high current levels which would

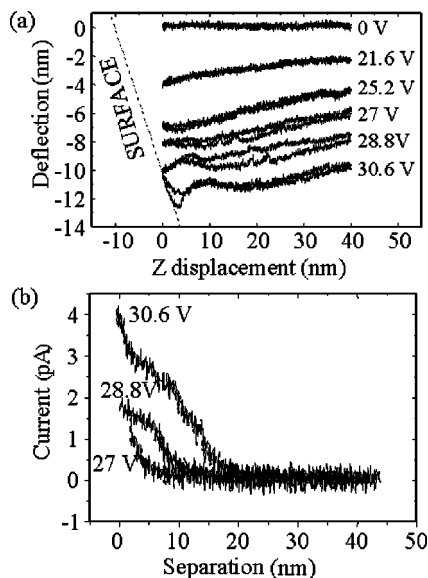


FIG. 3. (a) Set of high-voltage force-vs Z displacement curves performed in a way that the tip does not make mechanical contact with the surface. Tip velocity during the approach/retract excursion is 80 nm/s. (b) Current dependence of the approach curves as a function of tip-surface separation. The tip-surface separation has been obtained from the curves of Fig. 3(a).

obscure the phenomena and produce undesirable effects like surface breakdown at these high voltages. Figure 3(b) is the current dependence versus tip-sample separation, s . Although the applied voltage is considerable, the measured currents remain small. Thus, we are able to observe meniscus formation, the tip-sample distance at which current starts to flow, and the meniscus conductivity as a function of tip-sample separation. The current versus separation curves show a nonmonotonous behavior with regions of linear dependence of current on tip-sample distance. In addition, it is remarkable that the current during the approach and retraction part of the curves is very similar. Both phenomena indicate that the water meniscus dominates the flowing of current, and that the geometry of the meniscus determines the level of current achievable. If an ohmic conductivity for the water meniscus is assumed, then linear current dependence with tip-sample separation would indicate that the change of the meniscus diameter dominates the change of current observed when approaching the tip toward the sample. Experiments performed on H-passivated silicon (hydrophobic surface) show a different behavior: The dependence of current with tip-sample separation is exponential, consistent with the absence of a spontaneously formed water meniscus. More experiments under controlled humidity conditions are presently underway in order to analyze meniscus conductivity in a systematic manner. We observe that when the applied voltage is 30.6 V significant current flows through the meniscus, even at tip-sample separations as large as 20 nm. This is consistent with the fact that oxidation can be induced at large tip-sample separation.¹⁰

This work has been partially funded by Project DPI2000-0703. One of the authors (F.P.M.) acknowledges support from the Generalitat de Catalunya. Another (J.A.D.) acknowledges support from Jack Martinez and Steve Knight of the NIST Office of Microelectronics Programs.

¹J. A. Dagata, J. Schneir, H. H. Harary, C. J. Evans, M. T. Postek, and J. Benett, *Appl. Phys. Lett.* **56**, 2001 (1990).

²R. Held, T. Heinzel, P. Studerus, K. Ensslin, and M. Holland, *Appl. Phys. Lett.* **71**, 2689 (1997); K. Matsumoto, Y. Gotoh, T. Maeda, J. A. Dagata, and J. S. Harris, *ibid.* **76**, 239 (2000).

³T. Onuki, T. Tokizaki, Y. Watanabe, T. Tsuchiya, and T. Tani, *Appl. Phys. Lett.* **80**, 4629 (2002).

⁴G. Abadal, Z. J. Davis, A. Boisen, F. Pérez-Murano, X. Borrís, and N. Barniol, *Probe Microsc.* **2**, 121 (2001).

⁵J. A. Dagata, T. Inoue, J. Itoh, K. Matsumoto, and H. Yokoyama, *Appl. Phys. Lett.* **73**, 271 (1998).

⁶K. Morimoto, F. Pérez-Murano, and J. A. Dagata, *Appl. Surf. Sci.* **158**, 205 (2000).

⁷F. Pérez-Murano, K. Birkelund, K. Morimoto, and J. A. Dagata, *Appl. Phys. Lett.* **75**, 199 (1999).

⁸J. A. Dagata, F. Pérez-Murano, G. Abadal, K. Morimoto, T. Inoue, J. Itoh, and H. Yokoyama, *Appl. Phys. Lett.* **76**, 2710 (1998).

⁹F. Pérez-Murano, G. Abadal, N. Barniol, X. Aymerich, J. Servat, P. Gorostiza, and F. Sanz, *J. Appl. Phys.* **78**, 6797 (1995).

¹⁰R. García, M. Calleja, and F. Pérez-Murano, *Appl. Phys. Lett.* **72**, 2295 (1998).

¹¹P. Avouris, T. Hertel, and R. Martel, *Appl. Phys. Lett.* **71**, 285 (1997).

¹²T. G. Ruskell, J. L. Pyle, R. K. Workman, X. Yao, and D. Sarid, *Electron. Lett.* **32**, 1411 (1996).

¹³R. García, M. Calleja, and H. Rohrer, *J. Appl. Phys.* **86**, 1898 (1999).